



# Production of PLA-based AgNPs-containing nanofibers by electrospinning method and antibacterial application

Tansu Saygılı<sup>1</sup> · Havva Tutar Kahraman<sup>1</sup> · Gülsüm Aydın<sup>2</sup> · Ahmet Avcı<sup>3</sup> · Erol Pehlivan<sup>1</sup>

Received: 9 May 2023 / Revised: 3 August 2023 / Accepted: 14 August 2023

© The Author(s), under exclusive licence to Springer-Verlag GmbH Germany, part of Springer Nature 2023

## Abstract

Nanobiotechnology has achieved great advances in the field of scientific research in past years. Nanoparticles (NPs) with diameters ranging from 1 to 100 nm are the focus of nanotechnology. Green synthesis of encapsulated silver nanoparticles (eAgNPs) was carried out by using *Solidago virgaurea* L. (SvL) and *Tussilago farfara* L. (TfL) extract as reducing/protecting agent. An UV–vis spectrophotometer was used to determine the optimal conditions to produce eAgNPs from plant extracts, including pH, temperature, plant extract, and mixing times. The optimal conditions for AgNPs synthesis from the SvL plant and TfL plant were (1:1) extract-AgNO<sub>3</sub>, 24 h mixing time, and a temperature of 25 °C. SEM, TEM, FTIR, and UV–Vis Spectrophotometer analyses were carried out to ascertain the surface characterization and structural properties of eAgNPs and the nanofibrous mats' physico-chemical characteristics. The results of the analysis revealed that the eAgNPs are nanosized and contain silver. eAgNPs-doped nanofiber production from polylactide acid (PLA) polymer was realized by electrospin method. The required production parameters for the electrospinning method of producing PLA-based nanofibers were investigated. Nanofiber was produced by combining 0.5 and 1% AgNPs in an 8% PLA solution. The biological effects of the developed PLA@eAgNPs nanofibrous mats were examined in vitro. The antibacterial activity of nanofibers against *E. coli* was determined using the agar diffusion method. eAgNPs and PLA-based nanostructured materials are suggested as bioactive coatings capable of preventing the development of microbial population on surfaces relevant to healthcare.

**Keywords** Green synthesis · Antibacterial · Electrospin · Silver nanoparticles · Polylactic · Acid · Nanofiber

Extended author information available on the last page of the article

## Introduction

Today, nanoscience and nanotechnology are gaining popularity due to their significant impact on various fields such as energy, medicine, the pharmaceutical industry, electronics, and aerospace. Substances exhibit different properties at the nanoscale than at the macroscale due to quantum effects. The search for new, powerful antibacterial agents and their application in medicine are time-consuming, labor-intensive, and extremely expensive operations [1]. The size of nanoparticles (NPs) is affected by production parameters such as reaction temperature, reaction time, and pH. Application of NPs on the industrial scale is increasing quickly due to their unique and improved features based on size distribution and morphology. The use of various microorganisms, biological organisms, and extracts of various plants may be an alternative to physicochemical methods in eco-friendly and green synthesis [2]. AgNPs can kill bacteria and destroy distinct species of bacteria, viruses, and fungus due to the improvement of Ag's antimicrobial, antifungal, and antiviral activities at the nanometer scale [3]. Recently, AgNPs have been used on a large scale in field of the biology, chemistry, medicine, and physics due to their stability unique behavior at the nano-level [4].

The biological molecules are assembled in a carefully controlled manner to make them appropriate for the synthesis of metallic NPs, which has been discovered to be reliable and environmentally sustainable [5]. NPs can be created using a variety of methods, including chemical, physical, and biological ones. Although the chemical method of preparation involves a relatively short time for the biosynthetic pathways of a large quantity of nanomaterials, capping agents are required for the size stabilization of the NPs. The chemicals used in the production and destabilization of NPs are poisonous and produce unfriendly contaminants. The growing interest in biological approaches that do not use toxic chemicals as byproducts stems from the need for environmentally non-toxic synthetic methods for production of NPs. As a result, there is a growing demand for "green chemistry" [6] and green synthesis of nanomaterials has recently piqued the interest of researchers due to its lower toxicity to the environment and ease of production. Capping agents have been used to keep the size of NPs stable. The advancement of green NPs synthesis is an important branch of nanotechnology. The use of bioactive molecules such as microorganisms, plant extract, and plant biomass or waste in the synthesis of AgNPs may be an eco-friendlier alternative to chemical and physical production techniques.

Plants are a better system for synthesizing NPs because they are free from hazardous chemicals and contain natural capping agents. Furthermore, the use of plant extracts reduces the cost of microorganism isolation and pure culture, improving the cost-competitive effectiveness of microorganism-based production of NPs [6]. Because of their significant pharmacological properties, which include antimicrobial, antibacterial, anti-inflammatory, immunomodulatory, and excellent durability in severe conditions, biopolymers constituting nanoparticles of metals like silver and copper have recent times received the most focus [7, 8].

The synthesis of metallic NPs using different plants and their own extracts can sometimes be more beneficial than other biological synthesis processes involving the extremely complex methods of preserving microbial cultures [9, 10]. Many such tests were done, such as the synthesis of different metal NPs using fungi such as *Penicillium* sp. [11] and bacteria such as *Bacillus subtilis*, have already begun [12]. Furthermore, the effectiveness of the antimicrobial property is proportional to the size of the NPs. Because of the equivalent silver mass content, the tiny particles have stronger antibacterial properties.

Along with quick advancement in nanofiber synthesis and characterization during the past decade, significant work has been done to investigate potential functional applications of nanofibers, such as energy generation and storage, water and environmental treatment, medical applications, and biomedical engineering [13, 14]. The development of such hybrid materials, including the direct production of AgNPs in polymer matrices, has been quite active. Nanofibers are formed using methods such as drawing, phase separation, self-adhesion, chemical vapor deposition, nanopattern, melt spraying, and laser evaporation [15]. PLA is a biobased polymer that has recently gained prominence due to its advantageous properties, ease of processing, and comparatively higher supply when compared to certain other widely used thermoplastic polyesters [16–18]. Starch from natural materials, such as maize, wheat, sugar cane, and sugar beets, is used to make PLA. These benefits allow for the use of PLA in a spectrum of uses, especially in biomedical, food, and beverage, 3D printing, tissue engineering, and packaging industries [19]. The elastic modulus, elongation during break, and biodegradation rate of PLA are all higher.

Electrospinning is an extremely versatile technique that combines the use of two techniques, electrospray and spinning [20, 21]. The key idea behind the electrospinning method is to start creating nanofibers by spraying a polymer solution from a needle with an electrical charge. The resulting polymer jet is pulled from the tip of the needle to the collector by integrating the electrodes of a power source and varying the strength of the electric field between them. AgNPs were used to strengthen the PLA, a biopolymer. The solution contains PLA and AgNPs evaporate, causing the fibers to accumulate on the collector. The fibers' diameters range from micrometers to nanometers. The process parameters can be changed to change the diameter of the fibers [22]. The manufacture of microbial-resistant nanomaterials has garnered a lot of interest in preventing pathogenic bacteria from growing on substrate surfaces to improve the care for public health. We produced eco-friendly AgNPs for maybe the first time in this study by using herbs extract as a reducing and stabilizing agent, and we used them as a secure solid catalyst.

## Material and methods

### Materials

Several chemicals, reagents and solvents were purchased and used directly in the green synthesis, characterization, and implementation of eAgNPs in the research.

Dichloromethane (DCM), N, N-dimethylformamide (DMF) and  $\text{AgNO}_3$  were obtained from Sigma Aldrich Company. As a solvent, dichloromethane from VMR Chemicals was employed. PLA polymer was obtained from Esun company in filament form. All standards and solutions were created by dissolving the required amounts in ultrapure water. Every experiment relevant to the fiber synthesis process was conducted at room temperature.

### **Preparation of SvL and Tfl plants extract**

The SvL and Tfl herbs were gathered from a mountainous area in Hadim, Turkey, and dried in ambient sunlight. These plants were ground into powder into a fine powder using a mortar and pestle. 1000 ml of water and 10 g of herbs were boiled at 60 °C for 30 min. Using a magnetic stirrer rotating at 300 rpm, the herb extracts were mixed with 0.01 M  $\text{AgNO}_3$  in a 1:1 ratio over the period of 24 h in a darkly lit condition. The production of eAgNPs was accomplished using this supernatant. The precipitated eAgNPs were then put into petri plates for drying after the solution phase had been separated by centrifugation. The precipitated eAgNPs were removed from the petri plates and saved for the experiments.

### **Characterization of synthesized eAgNPs**

Spectrophotometer (Shimadzu UV-1700) was used to optimize different synthesis parameters such as precursor salt concentration, extract volume, pH, stirring speed and temperature effect under appropriate conditions. UV–Visible analysis was performed between 200 and 800 nm. A Bruker Vertex-70 Fourier transform infrared spectrophotometer (FTIR) was used for analysis to investigate the functional groups of the produced eAgNPs. Using an EDX detector connected to the SEM (HITACHI SU5000 Model and ZEISS EVO LS10 Model), EDX analysis was carried out to observe the elemental composition that indicates the distribution of elements in eAgNPs. Using the JEOL-Jem 2100 Model of transmission electron microscopy (TEM), morphological studies for eAgNPs were carried out.

### **Determination of parameters affecting AgNPs synthesis**

The pH, mixing time, temperature, and ratios of 0.01 M  $\text{AgNO}_3$  to plant extract that are necessary for the optimum synthesis of eAgNPs were all examined in various combinations. Data analysis was used to identify the ideal synthesis conditions for two plant species. The ideal pH for the synthesis of AgNPs was established by mixing plant extract with 0.01 M  $\text{AgNO}_3$  (1:1 ratio) for 24 h. HCl and NaOH were used to adjust the pH of the solution to 3, 5, 7, 9, and 11.  $\text{AgNO}_3$  (0.01 M) was applied to the plant extract at a 1:1 ratio for 24 h at 4 °C, 25 °C, 40 °C, and 60 °C. The chosen

plant extract was combined in a magnetic stirrer at 300 rpm for 1 min, 10 min, 30 min, 1 h, 2 h, 3 h, 5 h, 6 h, and 24 h after being exposed to 0.01 M  $\text{AgNO}_3$  in a (1:1) ratio. 10 ml of plant extract were combined with 2.5, 4, 5, 6, 7, 8, 9, and 10 ml of 0.01 M  $\text{AgNO}_3$  for 24 h. The ideal production values were then provided after analyzing each of these changes to manufacture eAgNPs.

### Nanofiber production by electrospin method

The PLA polymer was used to construct nanofibers, and due to the solubility of PLA, the solvents DCM and DMF were chosen. The mats were produced by mixing 1:4 ratios of PLA polymer with 8% of DCM-DMF solvents with a magnetic stirrer for 6 h at a speed of 500 rpm to obtain a homogeneous solution. eAgNPs were added to the polymer solution to give the generated nanofibers antibacterial abilities. To prevent photo-activation, the solution was shielded by enclosing the container in aluminum foil. It was then incubated at room temperature for 24 h. The yellowish tone of the solution turned into a reddish-brown color. The bioreduction process was observed after the PLA solution was treated with eAgNPs made from the extract of SvL and TfL herbs at 0.5 and 1% ratios, respectively. Further research was done on how eAgNPs affected antibacterial activity.

The electro spinning syringes were used in combination via electro spinning device with controlled doses of the PLA polymer solution and eAgNPs. Pump-connected syringes had a 15 cm space between them and the collector. The collector has a foil covering made of aluminum. Electrospinning was carried out in a rotating drum collector at 30 kV and 1 ml/h flow rate. The mats made of PLA were prepared using the two different eAgNPs in an electrospinning unit. The nanofibers produced using this method were detached from the aluminum foil using scissors. Pumping eAgNPs-doped PLA polymer solution from syringes to the aluminum foil-covered collector situated at the distance specified by the electric current made it simple to obtain the nanofibers on the collector. All steps applied to obtain eAgNPs-doped nanofibers in the experimental section are given in Fig. 1.

### Antibacterial activity of electrospun nanofibers

Antibacterial activities of neat PLA nanofibers and PLA nanofibers doped with eAgNPs were examined against Gram-negative *E. coli* (ATCC25922) bacteria via disk diffusion method [23]. *E. coli* bacterial suspensions were diluted to  $10^6$  CFU/mL in saline. After dilution, 100  $\mu\text{l}$  of the bacterial suspension was completely dispersed on Nutrient agar plates. Circular samples of 9 mm in diameter were prepared from each type of PLA nanofiber to evaluate the antibacterial activity. The samples were exposed to UV light for 10 min for sterilization. Each nanofiber sample was placed on the inoculated petri plates and incubated at 37 °C for 24 h. At the end of the incubation period, the zones of inhibition around the circular samples were visually inspected and the zone diameters were measured.

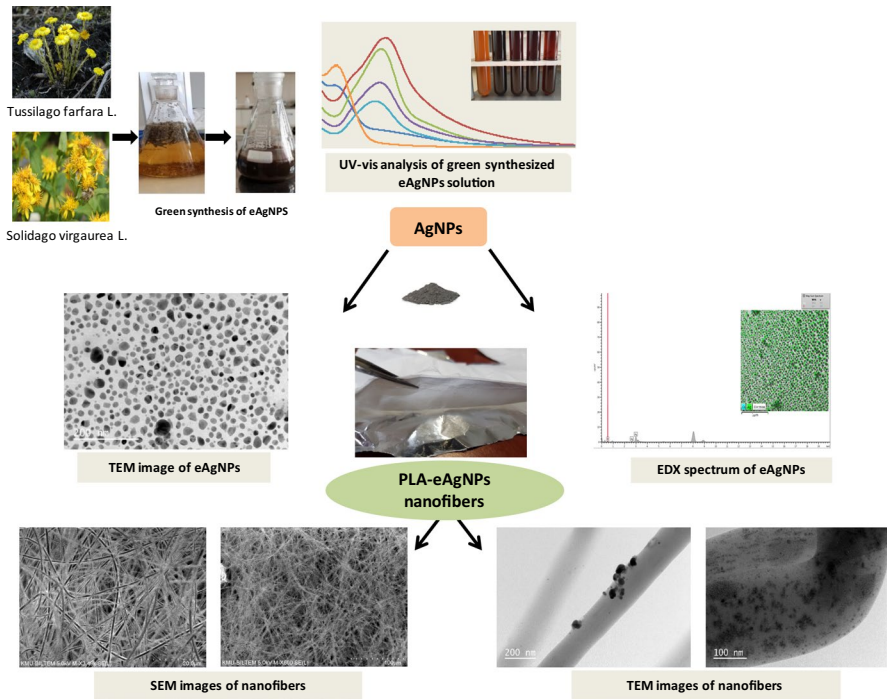
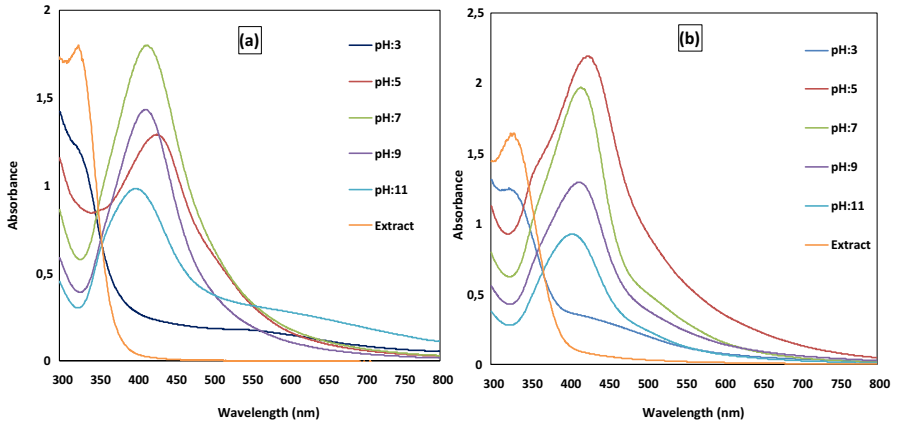


Fig. 1 Experimental steps of production of eAgNPs-doped nanofibers

## Results and discussion

### UV-vis spectroscopy characterization of electrospun nanocomposite fibers and synthetic eAgNPs

The size and shape of nanostructured materials can be controlled by the electro-optic response of metallic NPs [24]. As a research instrument, UV-vis spectroscopy can be utilized to optimize various reaction parameters during the synthesis of nanoparticles. UV-vis spectroscopic parameters were recorded to optimize several reaction factors, such as pH efficiency, reaction retention time, temperature influence, and extract volume on the production of small size and shape of eAgNPs. The shape of the produced eAgNPs was controlled by pH research. It is true that several factors, including particle size, shape, aggregation state, capping agent, and particle assembly composition, have an impact on the fixed location of eAgNPs peak [25]. The morphological characteristics of nanoparticles are significantly influenced by pH, a critical parameter. The pH of the solution phase was set to be between 3 and 11. Due to the presence of the bluer shifted band in the spectrum portfolio and the pH spectral profile of the eAgNPs made from SvL extract, pH-7 at 430 nm was suitable for the presence of new size eAgNPs, as shown in Fig. 2a. An inset figures of these characteristics showed that neither a color nor a band for current development could be seen in the more acidic



**Fig. 2** pH optimization study of AgNPs synthesis with SvL extract (a) and with TfL extract (b)

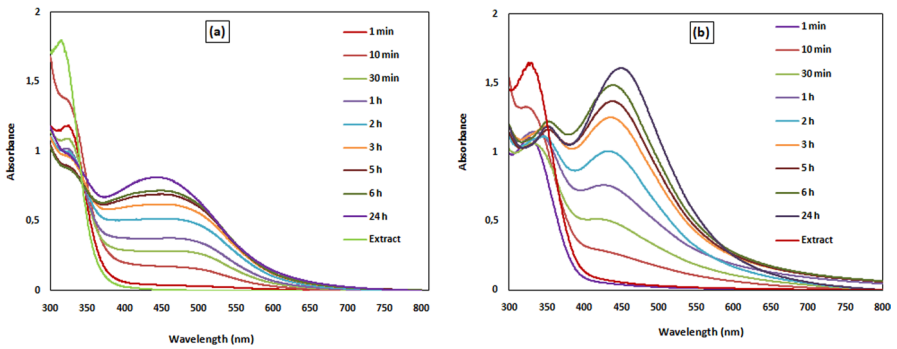


**Fig. 3** Time optimization study of eAgNPs synthesis with SvL extract (a) and with TfL extract (b)

area. The optimum pH value was 5.0 in the synthesis of eAgNPs with TfL extract (Fig. 2b).

According to research on the effect of time on the synthesis of green eAgNPs, standard laboratory temperature was excellent to produce small-sized eAgNPs, as depicted in Fig. 3. An inset image based on color change in Fig. 3. shows that increasing the time improves the band intensity of eAgNPs with blue shift.

The findings of optimizing the influence of temperature on the creation of eAgNPs showed that room temperature was suitable for the formation of small size eAgNPs, as shown in Fig. 4. Figure 4 shows that higher temperature tends to increase the band intensity of eAgNPs with blue shift, which was confirmed by an inset image based on color change. When compared to various temperature values in Fig. 4., it was established that carrying out the synthesis operations of eAgNPs with SvL extract under 25 °C was appropriate with an absorbance value of 1.65 at a wavelength of 450 nm. UV–vis spectrophotometer yielded an absorbance value

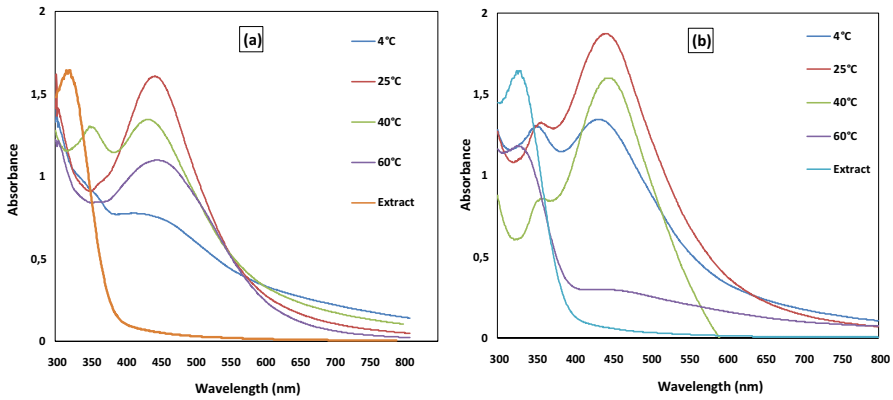


**Fig. 4** Effect of temperature on the formation of eAgNPs with SvL extract (a) and with TfL extract (b)

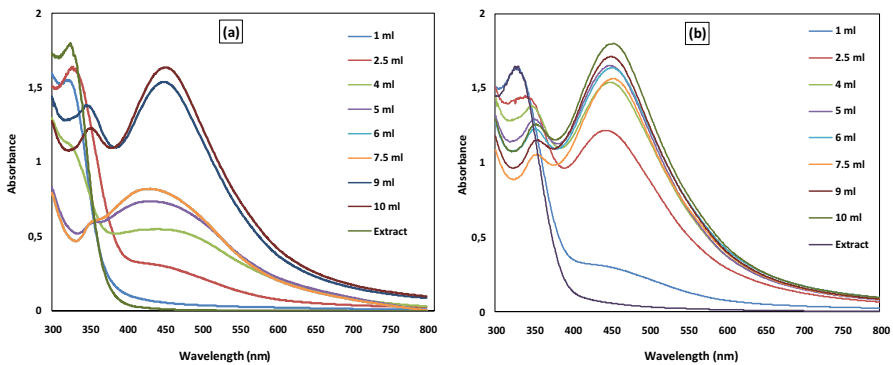


**Fig. 5** Plant extract/AgNO<sub>3</sub> optimization study of eAgNPs synthesis with SvL extract (a) and with TfL extract (b)

of 1.83 at 450 nm and 25 °C or determining the optimal temperature for eAgNPs synthesis with TfL.

The SvL and TfL extract volume was adjusted, according to the UV–vis profile in Fig. 5. Figure 5 shows that higher extraction volumes tended to increase the banding intensity from 1 to 10 ml of eAgNPs extract to adjust to produce small eAgNPs sizes. It was determined that using 1 ml SvL extract under 25 °C for the synthesis of eAgNPs was adequate with an absorbance value of 1.65 at a wavelength of 450 nm, which was indicative of a blue shift, when compared to other extract volumes in Fig. 5a. The UV–vis spectrophotometer produced an absorbance value of 1.85 at 450 nm and 25 oC for the eAgNPs production using 1 ml TfL Fig. 5b.



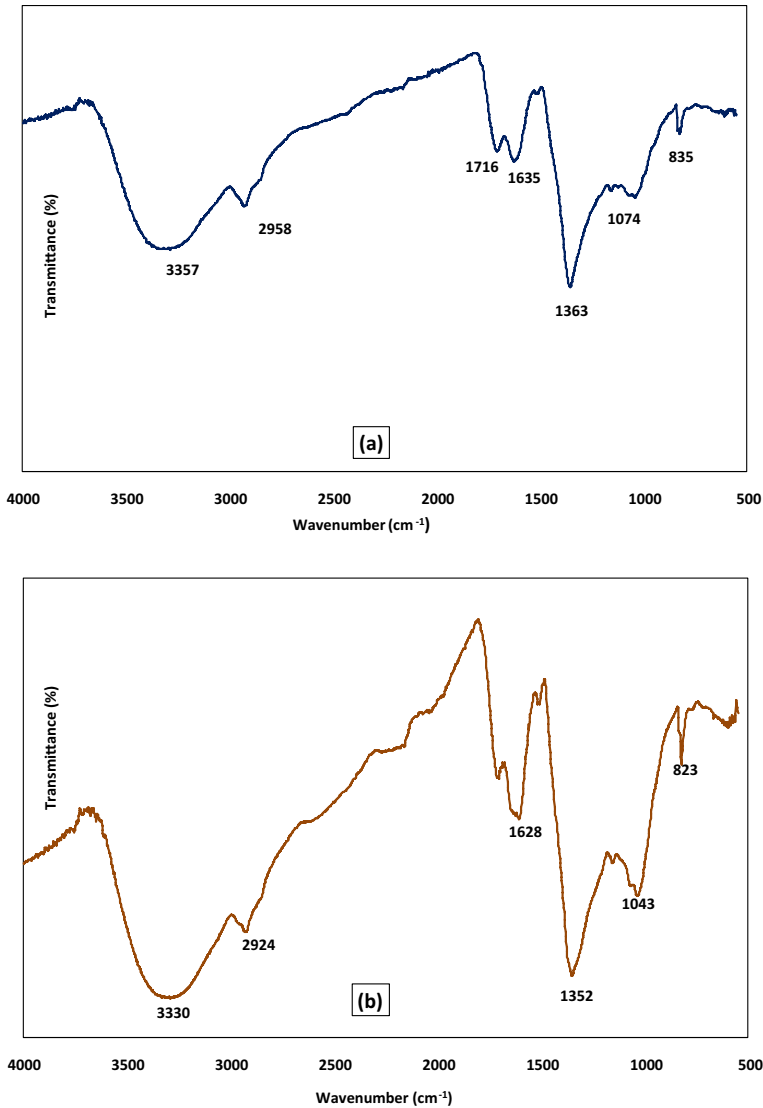


Fig. 6 FTIR results of AgNPs synthesis with SvL extract (a) and with TfL extract (b)

### Physicochemical analysis using FTIR spectroscopy

FTIR spectroscopic analyses were carried out to investigate the various interactions between SvL and TfL extract with AgNPs. FTIR spectroscopy revealed that there is interaction between the extract and the AgNPs. In the FTIR analysis results of AgNPs synthesized from SvL extract (Fig. 6a), the 3357 cm<sup>-1</sup> band corresponds to -OH stretching vibration caused by phenol compounds. The peak for the carbonyl group was obtained at 1716 cm<sup>-1</sup>. The carbonyl groups demonstrated the presence

of flavanones or terpenoids that are adsorbed on the surface of silver nanosized particles. The C–H stretching vibration is represented by the  $2958\text{ cm}^{-1}$  band. Carboxyl groups attached to the amide band are denoted by the abbreviation  $1635\text{ cm}^{-1}$  [25]. The C–N vibrations of aromatic amines are represented by the  $1363\text{ cm}^{-1}$  band [26]. The band at  $1074\text{ cm}^{-1}$  corresponds to C–N stretching vibrations of aliphatic amines. The spectrum of AgNPs synthesized from Tfl extract is also shown in Fig. 6b. C–OH vibrations that are often present in biogenic AgNPs are represented by the wavelength at  $1043\text{ cm}^{-1}$  in the FTIR spectrum of Tfl extract–AgNPs (Fig. 6b). The C–N vibrations of aromatic amines are represented by the  $1352\text{ cm}^{-1}$  band. The stretching vibrations of the carboxyl groups attached to the amide band are  $1628\text{ cm}^{-1}$ . The C–H stretching vibration is represented by the  $2924\text{ cm}^{-1}$ . The O–H stretching vibration caused by phenol compounds corresponds to the  $3330\text{ cm}^{-1}$  band. The peak appearing at  $1043\text{ cm}^{-1}$  is assigned for C–N stretching vibrations of aliphatic amines. Both plants' FTIR spectra agree with each other and with the literature [26]. Evaluation of the chemical composition of the surface of the silver nanoparticles indicated the involvement of amides, carboxyl, amino groups and poly phenols in the synthesized AgNPs. These organic compounds in plant extracts could attribute to the reduction of  $\text{AgNO}_3$  and the stabilization of AgNPs by the surface bound by the organic molecules. As a result, this analysis confirmed that both plant extracts have the ability to perform dual functions of reduction and stabilization of silver nanoparticles.

### TEM images of plant extract encapsulated eAgNPs

The sizes of AgNP encapsulated in extract SvL range from about 5 to 20 nm (Fig. 7a). eAgNP shapes vary from spherical to ovals. The average size of eAgNP is around 8 nm. The size of eAgNP produced with Tfl extract ranged from 5 to 25 nm (Fig. 7b). The average size of eAgNP is 18 nm. The shape of the eAgNP is oval and irregularly shaped close to oval.

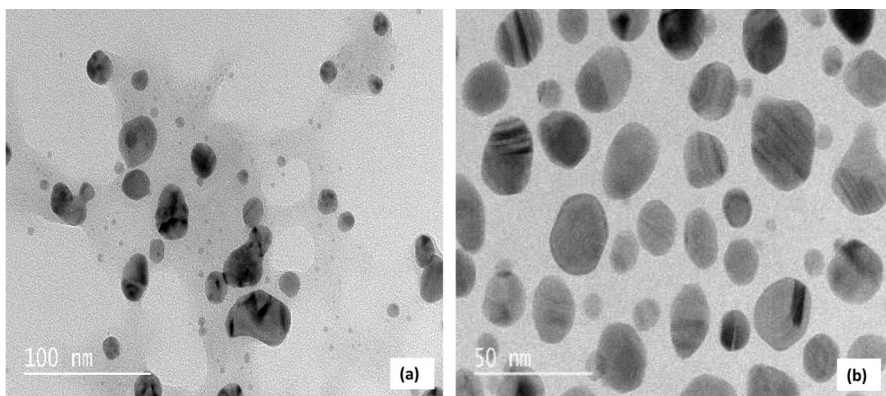


**Fig. 7** TEM images of SvL extract capped eAgNPs (a) and Tfl extract capped eAgNPs (b)

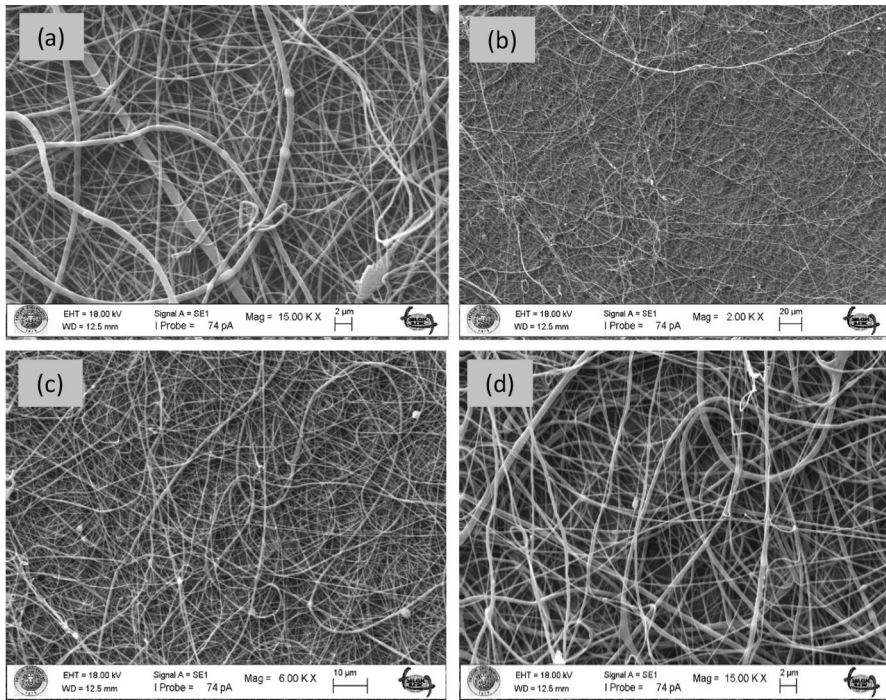


**Fig. 8** SEM images of PLA-based nanofibers with eAgNPs (0.5%) (**a**, **b**) and eAgNPs (1%) synthesized from SvL extract (**c**, **d**)

### Scanning electron microscopy (SEM) analysis and energy dispersive X-Ray spectroscopy (EDS)

The SEM analysis confirmed the presence, shape, and size of the nanoparticles in the fibers produced eAgNPs by SvL and Tfl extract (Figs. 8 and 9). By examining the SEM images, it is possible to evaluate the size and size distribution of the produced fibers. SEM images show that there are gaps between the nanofibers. The structure does not have a lot of beading. Nanofibers with diameters ranging from 85 to 470 nm have been discovered. The average diameter of the nanofiber was determined to be 327 nm. An increase in nanofiber diameter and a small amount of bead formation were observed as the particle amount increased. Nanofibers with diameters ranging from 140 to 600 nm are visible. It was discovered that the average nanofiber diameter was 335 nm.

In terms of application area, the structure with spaces between the fibers provides an advantage. While fibers with diameters ranging from 95 to 700 nm were observed, the average nanofiber diameter was determined to be 400 nm for SvL extract. There was no bead formation in the fibers. The diameter of the nanofiber increased in proportion to the number of nanoparticles added. The average nanofiber diameter of the structure's fibers was determined to be 490 nm. When compared to nanofibers containing 0.5% AgNPs, a more disordered structure was observed.

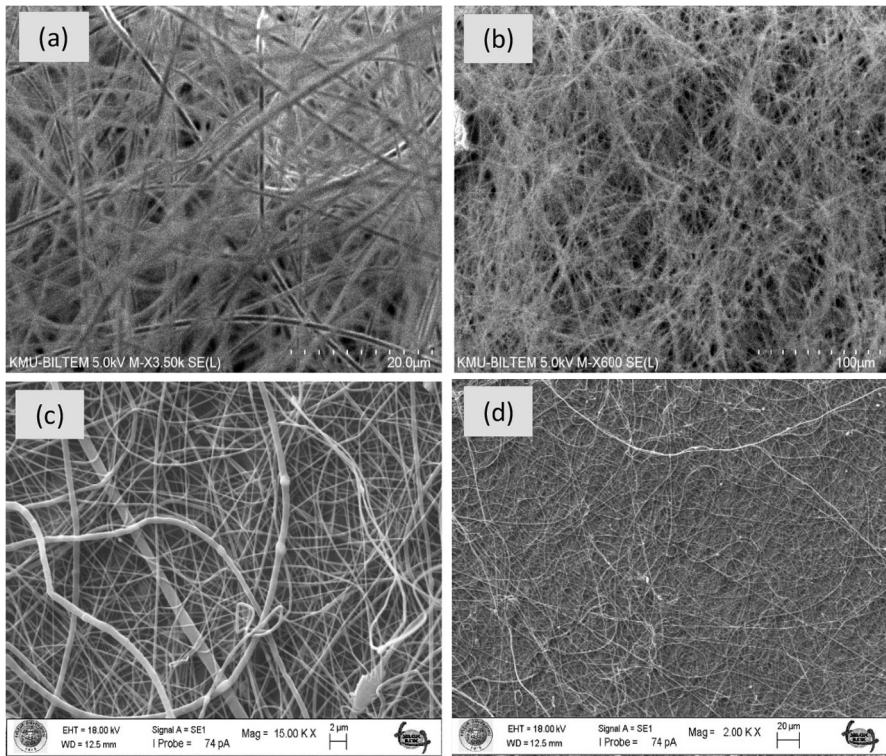


**Fig. 9** SEM images of PLA-based nanofibers with eAgNPs (0.5%) (**a, b**) and eAgNPs (1%) synthesized from TfL extract (**c, d**)

### Morphological analyses using transmission electron microscopy (TEM)

The results of the TEM analysis of the PLA@eAgNPs nanofibers produced from the SvL extract are shown in Fig. 10. The morphological features of eAgNPs generated from TfL extract were examined by TEM analysis, as seen in Fig. 10. The form of the eAgNPs is like a sphere. Particle aggregation is prevented when eAgNPs grow in the PLA polymer matrix. According to TEM images, the majority of the eAgNPs were monodispersed, spherical in shape, and ranged in size from 2 to 22 nm, with an average size of 9.5 to 9.8 nm. SvL extract eAgNPs (0.5%) are shown in Fig. 10a, b, and TfL extract eAgNPs (0.5%) are shown in Fig. 11a, b. The size distribution histogram of SvL-eAgNPs revealed that the eAgNPs have an average size of 10 nm with SvL extract and 12 nm with TfL extract. Small eAgNPs are readily apparent clinging to the surface of the fibers because of the green approach's coating of eAgNPs with biomolecules from the herb extract [27, 28]. The majority of the eAgNPs are well-distributed, with no agglomeration in solution and within the 3–21 nm range with SvL extract and 1.0% AgNPs and 2–22 nm with TfL extract and 1.0% AgNPs,



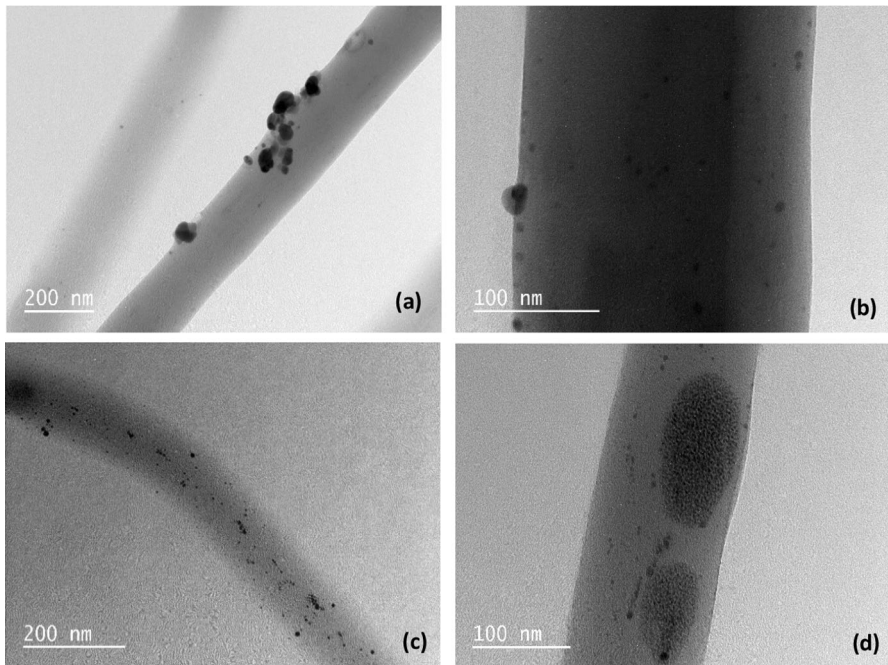


**Fig. 10** TEM images of PLA-based nanofibers with eAgNPs (0.5%) and eAgNPs (1%) synthesized from SvL (c, d)

according to the TEM micrograph of eAgNPs obtained in aqueous solution under normal conditions (Figs. 10c, d and 11c, d).

EDX analysis also was conducted to observe the elemental composition that indicates the distribution of elements in eAgNPs using an EDX detector connected to the SEM.

The EDX spectrum of eAgNPs presented in Fig. 12. verified the elemental composition that existed in plant and  $\text{AgNO}_3$ , revealing the strongest absorption band at 3 keV caused by the silver (Ag) region and weaker signals at 0.12, 0.20, and 0.26 keV from C, N, and O atoms, respectively.

### Antibacterial activity

AgNPs have been shown to affect both gram-positive and gram-negative bacteria and fungi equally, and they need to infiltrate the cellular membranes to exert their antimicrobial effects. AgNPs may adhere to the cell membrane's exterior surface, impinge on bacteria, and liberate silver ions. The basic antibacterial mechanism of AgNPs is focused on the suppression of protein biosynthesis, which is carried out by the 30 s subunit of the ribosome, and nucleic acid synthesis. Furthermore, this results in the production of reactive oxygen species [29]. It is possible to explain the hypothesized strategy as regards: The extraordinary reactivity of  $\text{Ag}^0$  to oxygen or

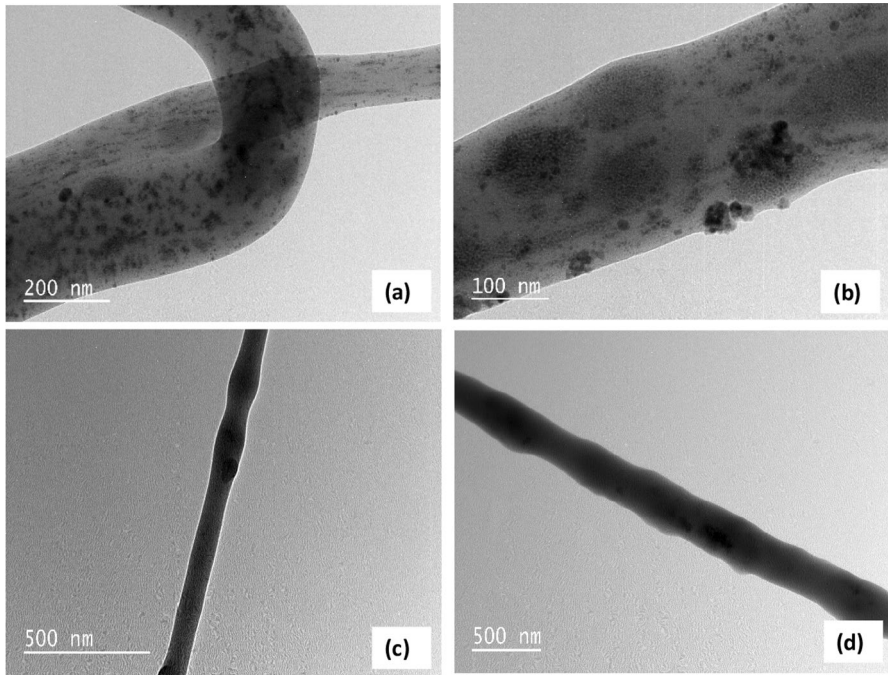


**Fig. 11** TEM images of PLA-based nanofibers with eAgNPs (0.5%) and eAgNPs (1%) synthesized from TfL (c, d)

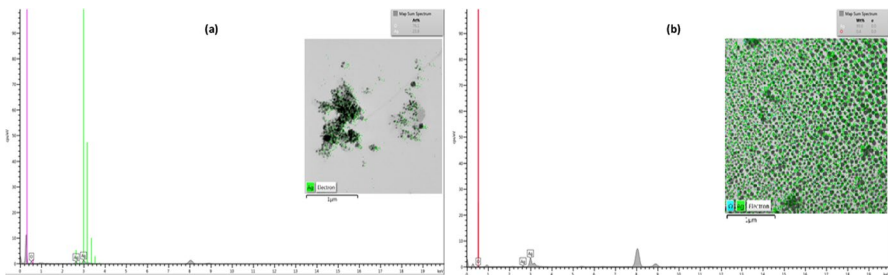


**Fig. 12** EDX spectra images of SvL extract capped AgNPs (a) and TfL extract capped eAgNPs (b)

its interaction with water molecules were the main causes of its conversion to  $\text{Ag}^+$  ions. The primary contributor to the antimicrobial activities was the strong affinity of  $\text{Ag}^+$  for phosphorus or sulfur. According to a theory,  $\text{Ag}^0/\text{Ag}^+$  potentially binds with the phosphate groups in DNA, inactivating DNA replication and inhibiting enzymatic activity [29].

The inhibitory zones of neat PLA nanofibers and PLA nanofibers doped with SvL and TfL eAgNPs are depicted in Fig. 13. Neat PLA nanofibers exhibited no antibacterial activity against the test bacterium. On the other hand, AgNP-containing nanofibers showed a dose dependent growth inhibiting effect. Although the

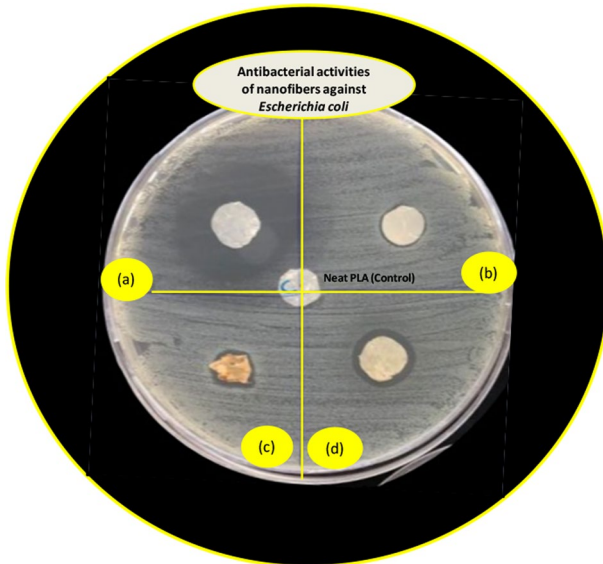


**Fig. 13** Inhibitory zones of PLA-based nanofibers with eAgNPs synthesized from TfL extract (1 and 0.5%) (a, b) and PLA-based nanofibers with eAgNPs synthesized from SvL extract (0.5 and 1%) (c, d)

nanofibrous mats capped with 0.5% AgNP gave poor inhibition zones, the nanofibers containing 1%AgNP showed good antibacterial activity. The antibacterial effect of the nanofiber doped with TfL encapsulated AgNPs was even more pronounced compared to SvL encapsulated AgNPs-containing nanofiber. There are several mechanisms reported to be responsible for the antibacterial activity of silver nanoparticles. They are suggested to interact with the bacterial membrane components and with phosphorus and sulfur containing compounds of macromolecules such as proteins and DNA [30, 31]. Attachment of the nanoparticles to the surface of the cell membrane disrupts the permeability of the membrane which is vital for cell survival. AgNPs can release silver ions and these ions once penetrated inside the cell can lead to generation of reactive oxygen species (ROS) and interact with the sulfur and phosphorus of DNA. Formation of ROS and modification of DNA may result in problems associated with DNA replication, cell division and even lead to cell death [32]. The intracellular damage caused by AgNPs depends on the particle size and shape [30].

According to the results obtained in this study, eAgNPs generated from TfL and SvL extract can be added to PLA nanofibers to successfully limit bacterial growth.

## Conclusion

PLA nanofibers containing silver were made sustainably. When AgNPs were produced using SvL, their size was decreased by using herb extract and then the PLA was supplemented with the developed eAgNPs (chemical approach). In this

research, a successful green chemistry approach was developed using SvL and TfL extract as a significantly reducing and stabilizing agent rather than toxic substances and organic solvent. The developed fabrication methodology was sustainable, more environmentally friendly, less costly, simpler, and much more effective. Various reaction variables, such as precursor salt concentration, volume of SvL and TfL extract, temperature effect on nanoparticle formation, and stirring rate, were optimized during the study. pH is an important factor that can have a significant impact on the production of NPs. pH was optimized in the research to evaluate small size nanoparticles by controlling size at the nm level. The green synthesized NPs were characterized using sophisticated analysis methods after they had been optimized. When compared to other plant extracts synthesized NPs, the synthesized eAgNPs were inherently stable and small. The biomedical field can utilize the PLA@eAgNPs fibers that were produced in this work.

## Declarations

**Conflict of interest** No potential conflict of interest was reported by the author(s). No funds have been used.

## References

- Herrmann J, Lukežič T, Kling A, Baumann S, Hüttel S, Petković H, Müller R (2016) Strategies for the discovery and development of new antibiotics from natural products: three case studies. *How Overcome Antibiotic Crisis: Facts, Challenges, Technol Future Perspect* 398:339–363
- Kanmani P, Rhim JW (2014) Physical, mechanical and antimicrobial properties of gelatin based active nanocomposite films containing AgNPs and nanoclay. *Food Hydrocoll* 35:644–652
- Shrivastava S, Bera T, Singh SK, Singh G, Ramachandrarao P, Dash D (2009) Characterization of antiplatelet properties of silver nanoparticles. *ACS Nano* 3(6):1357–1364
- Venkatesham M, Ayodhya D, Madhusudhan A, Santoshi Kumari A, Veerabhadram G, GirijaMangatayaru K (2014) A novel green synthesis of silver nanoparticles using gum karaya: characterization, antimicrobial and catalytic activity studies. *J Cluster Sci* 25(2):409–422
- Xu W, Jin W, Lin L, Zhang C, Li Z, Li Y, Li B (2014) Green synthesis of xanthan conformation-based silver nanoparticles: antibacterial and catalytic application. *Carbohydrate Polym* 101:961–967
- Darroudi M, Zak AK, Muhamad MR, Huang NM, Hakimi M (2012) Green synthesis of colloidal silver nanoparticles by sonochemical method. *Mater Lett* 66(1):117–120
- Demchenko V, Riabov S, Rybalchenko N, Goncharenko L, Kobylinskyi S, Shtompel V (2017) X-ray study of structural formation, thermomechanical and antimicrobial properties of copper-containing polymer nanocomposites obtained by the thermal reduction method. *Eur Polym J* 96:326–336
- Merki P, Long S, McInerney GM, Sotiriou GA (2021) Antiviral activity of silver, copper oxide and zinc oxide nanoparticle coatings against SARS-CoV-2. *Nanomaterials* 11(5):1312
- Velusamy P, Das J, Pachaiappan R, Vaseeharan B, Pandian K (2015) Greener approach for synthesis of antibacterial silver nanoparticles using aqueous solution of neem gum (*Azadirachta indica* L.). *Ind Crops Prod* 66:103–109
- Marsili E, Das SK (2016) Biosynthetic nanoparticles for biotechnological and biomedical applications. *Enzyme Microb Technol* 100(95):1–3
- Vidhu VK, Philip D (2014) Catalytic degradation of organic dyes using biosynthesized silver nanoparticles. *Micron* 56:54–62
- Kalwar NH, Sherazi STH, Khaskheli AR, Hallam KR, Scott TB, Tagar ZA, Soomro RA (2013) Fabrication of small l-threonine capped nickel nanoparticles and their catalytic application. *Appl Catal A* 453:54–59



13. Lim CT (2017) Nanofiber technology: current status and emerging developments. *Prog Polym Sci* 70:1–17
14. Keshavarz AH, Montazer M, Soleimani N (2020) In situ synthesis of polyamidoamine/ $\beta$ -cyclodextrin/silver nanocomposites on polyester fabric tailoring drug delivery and antimicrobial properties. *React Funct Polym* 152:104602
15. Schorr SJTSF (2007) Structural aspects of adamantane like multinary chalcogenides. *Thin Solid Films* 515(15):5985–5991
16. Sharif A, Mondal S, Hoque ME (2019) Polylactic acid (PLA)-based nanocomposites: processing and properties. *Bio-Based Polym Nanocompos: Preparat, Process, Propert & Perform* 2019:233–254
17. Shafiee Nasab M, Tabari M (2018) Antimicrobial properties and permeability of poly lactic acid nanocomposite films containing zinc oxide. *Nanomed Res J* 3(3):125–132
18. Liu C, Chan KW, Shen J, Wong HM, Yeung KWK, Tjong SC (2015) Melt-compounded polylactic acid composite hybrids with hydroxyapatite nanorods and silver nanoparticles: biodegradation, antibacterial ability, bioactivity, and cytotoxicity. *RSC Adv* 5(88):72288–72299
19. Babu RP, O'connor K, Seeram R (2013) Current progress on bio-based polymers and their future trends. *Prog Biomater* 2:1–16
20. Agarwal S, Wendorff JH, Greiner A (2008) Use of electrospinning technique for biomedical applications. *Polymer* 49(26):5603–5621
21. Song J, Kim M, Lee H (2020) Recent advances on nanofiber fabrications: unconventional state-of-the-art spinning techniques. *Polymers* 12(6):1386
22. Subbiah T, Bhat GS, Tock RW, Parameswaran S, Ramkumar SS (2005) Electrospinning of nanofibers. *J Appl Polym Sci* 96(2):557–569
23. Zivanovic S, Chi S, Draughon AF (2005) Antimicrobial activity of chitosan films enriched with essential oils. *J Food Sci* 70(1):M45–M51
24. Noguez C (2007) Surface plasmons on metal nanoparticles: the influence of shape and physical environment. *J Phys Chem C* 111(10):3806–3819
25. Guajardo-Pacheco MJ, Morales-Sánchez JE, González-Hernández J, Ruiz F (2010) Synthesis of copper nanoparticles using soybeans as a chelant agent. *Mater Lett* 64(12):1361–1364
26. Azizi M, Azimzadeh M, Afzali M, Alafzadeh M, Mirhosseini S (2018) Characterization and optimization of using calendula officinalis extract in fabrication of polycaprolactone-gelatin electrospun nanofibers for wound dressing applications. *J Adv Mater Proc* 6:31–38
27. Remya RR, Rajasree SR, Aranganathan L, Suman TY (2015) An investigation on cytotoxic effect of bioactive AgNPs synthesized using *Cassia fistula* flower extract on breast cancer cell MCF-7. *Biotechnol Rep* 8:110–115
28. Kumar PV, Pammi SVN, Kollu P, Satyanarayana KVV, Shameem U (2014) Green synthesis and characterization of silver nanoparticles using *Boerhaaviadiffusa* plant extract and their anti bacterial activity. *Ind Crops Prod* 52:562–566
29. Kumar B, Smita K, Cumbal L, Debut A (2014) Synthesis of silver nanoparticles using *Sacha inchi* (*Plukenetia volubilis* L.) leaf extracts. *Saudi J Biol Sci* 21(6):605–609
30. Mijakovic I, Petranovic D, Macek B, Cepo T, Mann M, Davies J, Vujaklija D (2006) Bacterial single-stranded DNA-binding proteins are phosphorylated on tyrosine. *Nucleic Acids Res* 34(5):1588–1596
31. Marambio-Jones C, Hoek EMV (2010) A review of the antibacterial effects of silver nanomaterials and potential implications for human health and the environment. *J Nanopart Res* 12:1531–1551
32. Morones JR, Elechiguerra JL, Camacho A, Holt K, Kouri JB, Ramirez JT, Yacaman MJ (2005) The bactericidal effect of silver nanoparticles. *Nanotechnology* 16(10):2346
33. Yin IX, Zhang J, Zhao IS, Mei ML, Li Q, Chu CH (2020) The antibacterial mechanism of silver nanoparticles and its application in dentistry. *Int J Nanomed* 15:2555–2562

**Publisher's Note** Springer Nature remains neutral with regard to jurisdictional claims in published maps and institutional affiliations.

Springer Nature or its licensor (e.g. a society or other partner) holds exclusive rights to this article under a publishing agreement with the author(s) or other rightsholder(s); author self-archiving of the accepted manuscript version of this article is solely governed by the terms of such publishing agreement and applicable law.

## Authors and Affiliations

**Tansu Saygılı<sup>1</sup> · Havva Tutar Kahraman<sup>1</sup> · Gülsüm Aydın<sup>2</sup> · Ahmet Avcı<sup>3</sup> · Erol Pehlivan<sup>1</sup>**

✉ Erol Pehlivan  
erolpehlivan@gmail.com

<sup>1</sup> Department of Chemical Engineering, Konya Technical University, 42079 Konya, Turkey

<sup>2</sup> Department of Biotechnology, Selcuk University, Konya, Turkey

<sup>3</sup> Department of Mechatronics Engineering, Karatay University, Konya, Turkey